Development and Evaluation of a Surrounding Vehicle Identification System for Mixed Traffic Cooperative Platooning

Zeyu Mu, S.M.ASCE[1]; Md Ashraful Imran, S.M.ASCE[2]; Sergei S. Avedisov, Ph.D.[3]; and B. Brian Park, Ph.D., M.ASCE[4]

Abstract: To facilitate cooperation among connected automated vehicles (CAVs), such as cooperative platooning or cooperative lane changes in mixed traffic comprising CAVs, connected human-driven vehicles (CHVs), and conventional (unconnected) human-driven vehicles (HDVs), an ego CAV needs to discern which surrounding vehicles are connected (CAVs or CHVs) and which are unconnected (HDVs). Therefore, this paper introduces a surrounding vehicles identification system (SVIS) designed to enable CAVs to identify the connectivity status of surrounding vehicles. Unlike a previously developed preceding vehicle identification system that only identifies the connectivity of its immediately preceding vehicle, the proposed SVIS generalizes this identification to nearby surrounding vehicles. Furthermore, the proposed SVIS significantly reduces the error in the connected vehicle identification by integrating distance and the magnitude of velocity for matching instead of distance-only matching used by the previous system. The SVIS is a must to enable CAVs to form platoons via lane changes after a connected vehicle is detected in an adjacent lane. We compared a newly proposed distance-plus-speed-matching approach with a previously developed distance-only-matching approach using Next Generation Simulation (NGSIM) data. Through comparison, the efficacy of the proposed distance-plus-speed-matching SVIS is demonstrated to be considerably superior to that of the distance-only-matching SVIS. Given that a reliable and robust method for identifying surrounding connected vehicles is key to the successful formation of cooperative adaptive cruise control (CACC) platoons and cooperative lane changes, the proposed distance-plus-speed-matching SVIS would help quickly and efficiently form platoons in a mixed traffic environment. **DOI: 10.1061/JTEPBS.TEENG-8496.** © *2024 American Society of Civil Engineers.*

Introduction

Mobility and safety are the two primary goals of current and future intelligent transportation systems. The connected and automated vehicle (CAV) is a product integrating emerging technologies and the automobile industry, which has shown promising potential to improve mobility and safety. Vehicle automation makes transportation systems more intelligent, safe, and reliable (Yao et al. 2020). Bajpai (2016) showcased the benefits of CAVs in increased capacity without raising delay times compared with unconnected automated vehicles.

Although the Society of Automotive Engineers' Level 5 (i.e., driverless cars) automation is probably still far away, today's vehicles are equipped with adaptive cruise control (ACC), which has features of Level 1 and partial Level 2 automation (Kim et al. 2013). In addition, the evolution of vehicle connectivity enables CAVs to collaborate in various traffic scenarios, promoting both vehicle safety and efficiency. Specifically, cooperative platooning, i.e., cooperative adaptive cruise control (CACC) (Milanes et al. 2014; Naus et al. 2010; Ploeg et al. 2011; Rajamani and Shladover 2001) and cooperative lane changes (Wang et al. 2016; Zheng et al. 2020) are expected to realize such benefits by cooperating with target surrounding connected vehicles via sensor detection and vehicle-to-vehicle (V2V) communication.

V2V communication allows CACC vehicles to travel stably in a platoon with time headways as low as 0.6 s, making it possible to increase the road capacity by two to three times compared with human-driven traffic (Lioris et al. 2017; Shladover et al. 2012). To enable cooperation, the ego vehicle must establish a V2V connection with the surrounding connected vehicle after the detection is made by the onboard sensor. Once the V2V connection is established, the communication IDs of the connected vehicles can be obtained by the ego vehicle. Thus, the identification of the target vehicle is a must to form CACC platoons or implement cooperative lane changes. Generally, the process of identifying the target vehicle involves the comparison of self-reported positions obtained by the Global Positioning System (GPS) and reported in V2V messages, such as the basic safety message and positions obtained by the ego vehicle through sensor measurements. Once the sensor-measured positions match the GPS-based positions, the vehicle is considered the target vehicle.

There have been several studies regarding connected vehicle identification for CACC. Many researchers assumed that all

[1]Graduate Research Assistant, Link Lab, Univ. of Virginia, 151 Engineer's Way, Charlottesville, VA 22904; Dept. of Systems and Information Engineering, Univ. of Virginia, 151 Engineer's Way, Charlottesville, VA 22904 (corresponding author). ORCID: https://orcid.org/0000-0003-0957-0061. Email: dwe4dt@virginia.edu

[2]Graduate Research Assistant, Dept. of Civil Engineering, Univ. of Texas at Arlington, Arlington, TX 76019. ORCID: https://orcid.org/0000-0003-2024-3280. Email: mxi3942@mavs.uta.edu

[3]Researcher, InfoTech Labs, Mountain View, CA 94043; Toyota Motor North America R&D, 1555 Woodridge Ave., Ann Arbor, MI 48105. Email: sergei.avedisov@toyota.com

[4]Professor, Link Lab, Univ. of Virginia, 151 Engineer's Way, Charlottesville, VA 22904; Dept. of Civil and Environmental Engineering, Univ. of Virginia, 151 Engineer's Way, Charlottesville, VA 22904; Dept. of Systems and Information Engineering, Univ. of Virginia, 151 Engineer's Way, Charlottesville, VA 22904. ORCID: https://orcid.org/0000-0003-4597-6368. Email: bp6v@virginia.edu

Note. This manuscript was submitted on January 3, 2024; approved on May 31, 2024; published online on September 28, 2024. Discussion period open until February 28, 2025; separate discussions must be submitted for individual papers. This paper is part of the ***Journal of Transportation Engineering, Part A: Systems***, © ASCE, ISSN 2473-2907.

CACC-capable vehicles would be easily distinguished from the surrounding vehicles because they travel in a single platoon (Milanes et al. 2014; Naus et al. 2010; Ploeg et al. 2011; Rajamani and Shladover 2001). In the 2011 Grand Cooperative Driving Challenge (GCDC), CACC platoons developed by different research groups were competing in performance. In this challenge, a blacklist in the vehicle's software was used to label the messages from vehicles in the other lane that did not belong to the same platoon (Geiger et al. 2012). This strategy would not be applicable in the real world. Furthermore, despite all of GCDC's vehicles being equipped with high-precision GPS, the vehicles could not identify their predecessor with 100% accuracy.

Chen and Park (2020) developed a preceding vehicle identification system (PVIS) under a fully connected vehicle environment. Their study used GPS/sensor errors, vehicle geometry, and radar measurements of actual preceding vehicles to calculate a dynamic search region. A fundamental limitation is that their PVIS assumed every vehicle is connected. However, in the near future, the traffic will be mixed, with both connected and unconnected vehicles. Motivated the prediction of the adoption rate of vehicle connectivity [i.e., 100% adoption is not likely until the 2040s in the US (Bansal and Kockelman 2017)], Chen and Park (2022) modified their PVIS to deal with a mixed traffic environment and successfully demonstrated it using NGSIM data. They found GPS requires an accuracy of 1 m to make 99th-percentile time consumption less than 10 s.

The results of Chen and Park (2022) indicated that the multipath bias of GPS could contribute to the misidentification of a connected preceding vehicle as an unconnected vehicle. A drawback of their research is that the algorithm does not consider target vehicles at nearby lanes, a must for cooperative lane changes and forming CACC with an adjacent lane's connected vehicle. Another drawback is that their algorithm showed a nonzero identification error (i.e., identifying an unconnected vehicle as a connected vehicle), which is not suitable for real-world implementation.

Thus, this paper proposes significantly enhancing the previously developed PVIS by expanding its capability to identify nearby surrounding vehicles and integrating both speed and distance in identifying target vehicles. As noted, expanding the connectivity identification to all nearby surrounding vehicles is necessary for the ego vehicle to subsequently cooperate with these surrounding vehicles. For example, it allows the ego vehicle to make lane-change decisions in case a CACC vehicle intends to join a connected vehicle on a nearby lane.

The rest of the paper is organized as follows: The second section describes the identification procedure in mixed traffic by using relative position and speed obtained from GPS and radar sensors. The third section describes the design of the surrounding vehicles identification system (SVIS), including the outline of the design goals, the derivation of the searching area, and the optimization of the SVIS parameters. In the fourth section, the performance of the proposed SVIS is evaluated with real-world vehicle trajectory data. In the fifth section, we present findings from our research and discuss the potential enhancements for future research.

Conceptual Identification Procedure

The following assumptions are made for this study:

- Connected vehicles are equipped with GPS receivers.
- The CAV is equipped with multiple radar sensors providing a 360° field of view.
- The effects of V2V packet loss on our SVIS are insignificant.

Before proceeding with the proposed enhancement, it is noted that the decision to add the GPS speed to the SVIS algorithm was made based on the following information. Studies found that the GPS speed estimation is far more accurate and less vulnerable to the multipath effect (Jain et al. 2021; Kubo 2009; Sadrieh et al. 2000; Serrano et al. 2004). Using speed in addition to distance to perform identification should improve identification accuracy. In this study, the term speed specifically denotes the longitudinal component of the vehicle's velocity because the lateral component is typically minor and deemed negligible for the purposes of matching analysis.

A conceptual SVIS procedure consisting of distance and speed matching, dubbed ds-SVIS, is formulated as follows:

1. The identification procedure starts when the ego vehicle detects surrounding vehicles within the radar's maximum detection range.
2. The ego vehicle measures each detected relative position and speed of the target vehicle via radar. For the proposed approach, i.e., ds-SVIS, a search region, A, around the radar-measured position and speed is defined as shown in Fig. 1(a).
3. At the same time, the ego vehicle receives standardized messages such as the Basic Safety Message (Deng et al. 2017; V2X Core Technical Committee 2016), which contains the GPS positions and speeds of remote connected vehicles, as shown in Fig. 1(b). The radar measurement of the target vehicle is compared with the GPS positions and speeds in the V2V messages from connected vehicles within the communication range. The nearby connected vehicles whose GPS positions and speeds fall within the search region defined in Step 2 are considered candidates.
4. Steps 2 and 3 are repeated n times, and the candidates for the target surrounding vehicle are determined by whose self-reported GPS position and speed are within Search region A in all n iterations of Steps 2 and 3.
5. In Step 4, if there is only one candidate, that candidate is considered as the target vehicle, and the identification procedure stops.
6. If there is no candidate, the identification procedure restarts at Step 1, and Steps 1–3 are repeated up to k times. If the system does not find any candidate for k consecutive times of identification, the procedure ends, and the system considers the target surrounding vehicle to be unconnected.
7. If there are multiple candidates, the process goes back to Step 1 and restarts Steps 1–3.

The entire procedure is shown in Fig. 2. This process indicates that Step 1 can be repeated at most k times, whereas Steps 2 and 3 can be repeated $n \times k$ times. Both n and k are optimized parameters, as detailed in the next section.

Research Method

Design Approach

Based on the PVIS procedure of Chen and Park (2022), the proposed ds-SVIS approach was redesigned to incorporate nearby surrounding vehicles and utilize both distance and speed measures. The most serious error is to engage in CACC (or a different cooperative driving algorithm as well as lane change) with a mistakenly identified preceding vehicle. Thus, the primary objective is to minimize the probability of misidentifying the target vehicle (i.e., identifying an unconnected vehicle as a connected vehicle). Such misidentification errors are referred to as a vehicle misidentification error. A low vehicle misidentification error probability

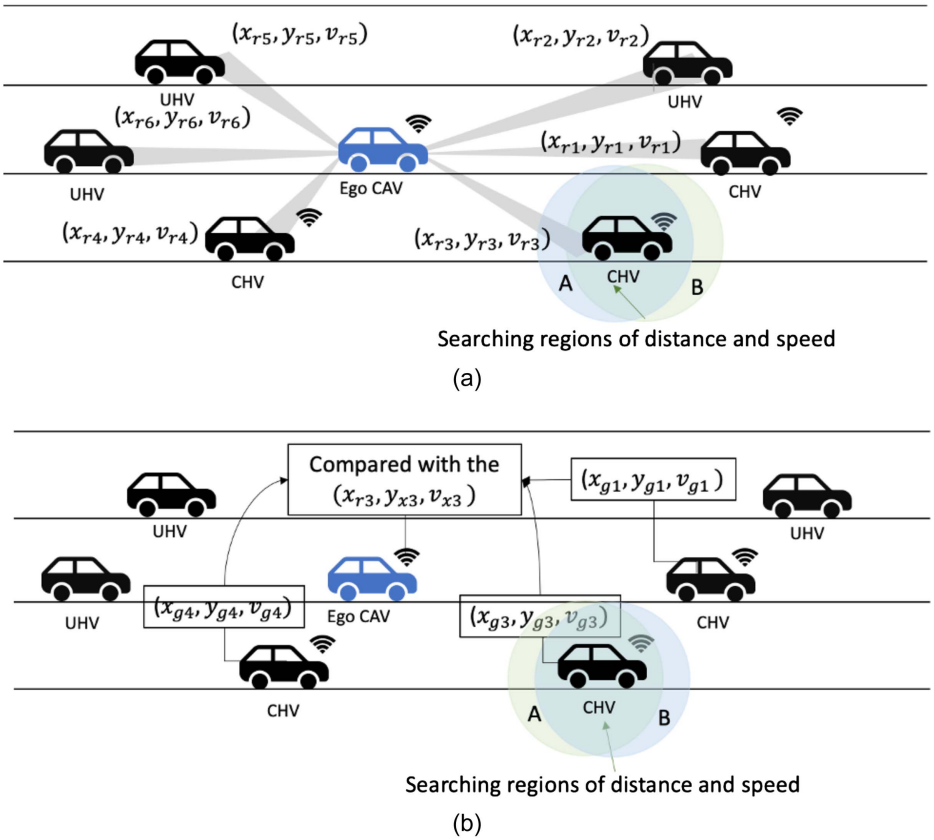

Fig. 1. (a) Search procedure with distance and speed; and (b) reception of GPS messages and comparison with the sensor measurement.

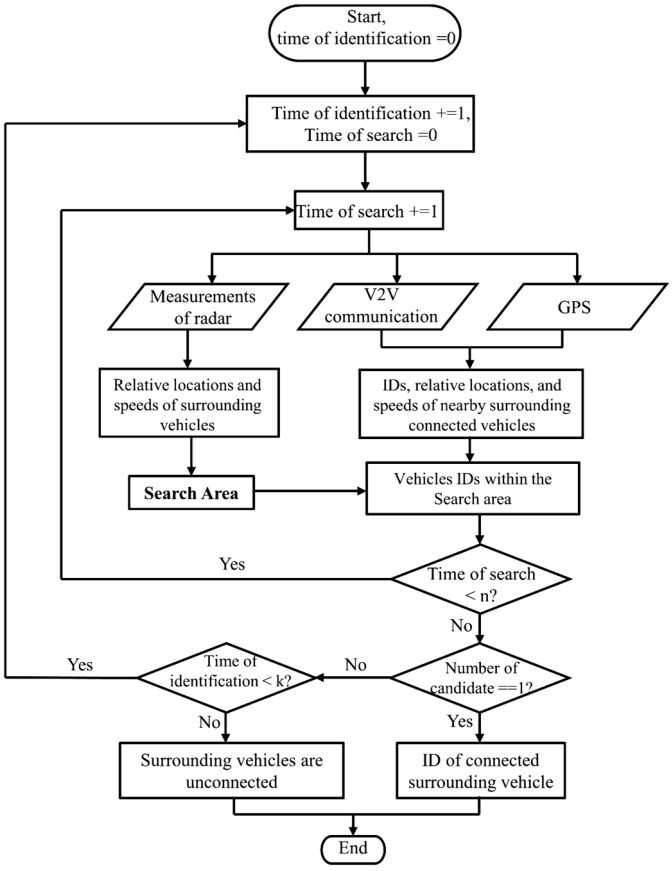

Fig. 2. Flowchart of the surrounding vehicles identification procedure.

ensures that the ego vehicle does not start cooperating with an irrelevant vehicle. The error of each surrounding target vehicle is calculated as follows:

$$E_r = \begin{cases} (1 - P_a)P_{irr} & \text{if the surrounding target vehicle is connected} \\ P_{irr} & \text{if the surrounding target vehicle is unconnected} \end{cases} \quad (1)$$

where P_a = probability for the target connected surrounding vehicle to be identified correctly; and P_{irr} = probability that an irrelevant surrounding vehicle is identified as the target connected vehicle. Table 1 lists all the symbols used in this study.

A secondary objective of the SVIS is to minimize misidentifying a connected vehicle as an unconnected vehicle, referred to as unusability error. In this case, the ego vehicle engages in a suboptimal control mode (for example, using adaptive cruise control rather than using cooperative adaptive cruise control). This is not as critical as attempting to cooperate with an irrelevant vehicle (as in the case of vehicle misidentification error). Under the assumption that the primary objective of $E_r \approx 0$ is achieved, the

Table 1. Optimal values of n, k, and α as a function of constraint parameters for the optimization problem

Target error rate	t_{max}	P_{min}	n	k	α	Target unusability rate
10^{-10}	35	0.95	40	7	0.0182	0.01033
10^{-8}			37	6	0.0165	0.00943
10^{-6}			21	8	0.0353	0.00621

unusability error $[U_r = (1 - P_a)(1 - E_r)]$, is approximated as $U_r \approx 1 - P_a$.

The last objective is to minimize the identification time consumption. The proposed approach implements multiple iterations to ensure both vehicle misidentification error and unusability error are minimized to acceptable levels. There is a clear trade-off between the acceptable errors and the identification time. To address these, an optimization approach was implemented to determine the weights between the competing objectives in the "Optimization Formulation and Optimized Parameters" section.

Search Region

Given that the proposed ds-SVIS searches all the nearby surrounding vehicles, the search region is expanded over the previous PVIS. Incorporating a speed measure in addition to distance added the search space and complexity in the optimization. The speed and distance measures are obtained from GPS and radar sensors, respectively. As mentioned in Step 2 of the proposed SVIS procedure, a search region includes an area around the detected nearby vehicles.

One condition to be a candidate for the surrounding target vehicle is given by a search region based on the position (i.e., longitudinal and lateral distance measure), which is defined as follows:

$$\left(\frac{ex_g - ex_r}{\delta_x}\right)^2 + \left(\frac{ey_g - ey_r}{\delta_y}\right)^2 < F^{-1}(\chi^2(2), 1 - \alpha_d) \quad (2)$$

where ex_r and ey_r = errors coming from the radar measurement of the surrounding vehicle's position in x- and y-directions; ex_g and ey_g = errors coming from the GPS measurement of the surrounding vehicle's position in x and y, respectively; and $F^{-1}(\chi^2(2), 1 - \alpha_d)$ = inverse cumulative distribution function of the Chi-square distribution with two degrees of freedom $[\chi^2(2)]$, evaluated at the probability values in probability $1 - \alpha_d$. Particularly, α_d is the probability that the actual surrounding connected vehicle is positioned out of the oval Region A defined by Eq. (2). As shown in Fig. 3, when $\alpha_d = 0.05$, then $F^{-1}(\chi^2(2), 1 - \alpha_d) = 5.99$.

In addition to the distance measure (i.e., position), the speed measure is considered. The measured speed by the radar and GPS are denoted as v_r and v_g, respectively. Given the actual vehicle speed as v, the following consider measured speeds with errors:

$$v_g = v + e_g \quad (3)$$

$$v_r = v + e_r \quad (4)$$

where e_g and e_r = speed errors due to GPS and radar, respectively.

The measurement errors of speed from radars and GPS were assumed to follow a normal distribution:

$$e_r \sim N(0, \sigma_r^2) \quad (5)$$

$$e_g \sim N(0, \sigma_g^2) \quad (6)$$

where σ_r and σ_g = standard deviations. Therefore

$$v_r - v_g = e_r - e_g \sim N(0, \delta_v^2) \quad (7)$$

where

$$\delta_v^2 = \sigma_r^2 + \sigma_g^2 \quad (8)$$

Then, δ_v^2 as a squared sum of one independent standard normal variable follows a Chi-square distribution with one degree of freedom. Similar to the position search region, the search region for (longitudinal) speed is defined by an inverse cumulative distribution function of the Chi-square distribution:

$$\frac{(e_r - e_g)^2}{\delta_v^2} < F^{-1}(\chi^2(1), 1 - \alpha_v) \quad (9)$$

where $F^{-1}(\chi^2(1), 1 - \alpha_v)$ = inverse cumulative distribution function of the Chi-square distribution with one degree of freedom, $\chi^2(1)$, evaluated at the probability values in probability $1 - \alpha_v$. Particularly, α_v is the probability that the actual surrounding connected vehicle is positioned outside the Region B defined by Eq. (9). As shown in Fig. 3, when $\alpha_v = 0.05$, then $F^{-1}(\chi^2(1), 1 - \alpha_v) = 3.84$.

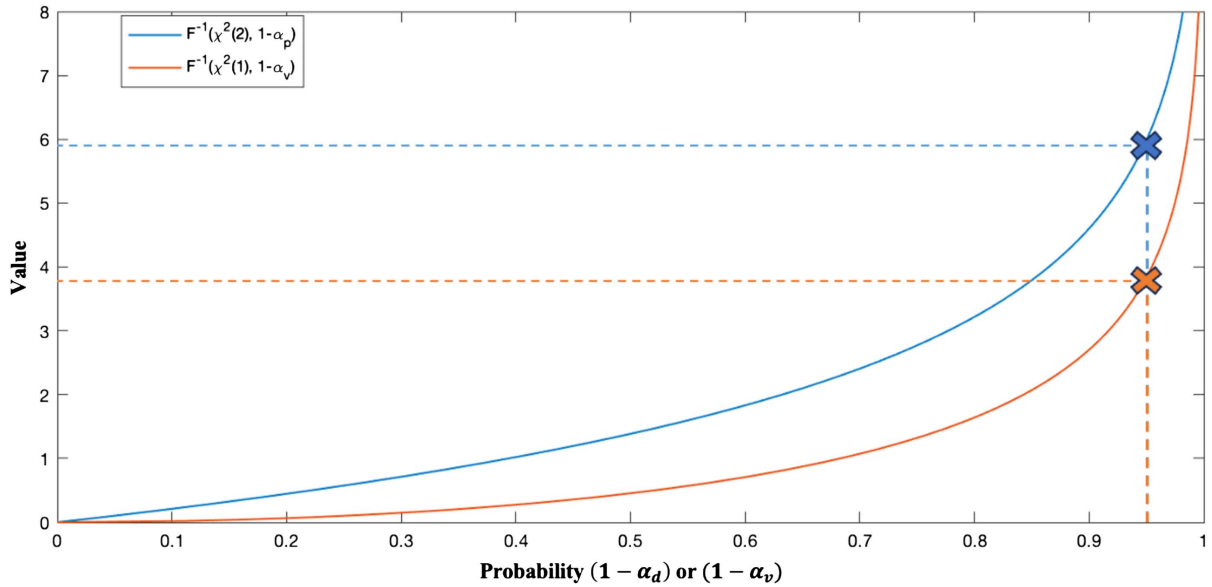

Fig. 3. Inverse cumulative distribution function of the Chi-square distribution.

J. Transp. Eng., Part A: Systems, 2024, 150(12): 04024078

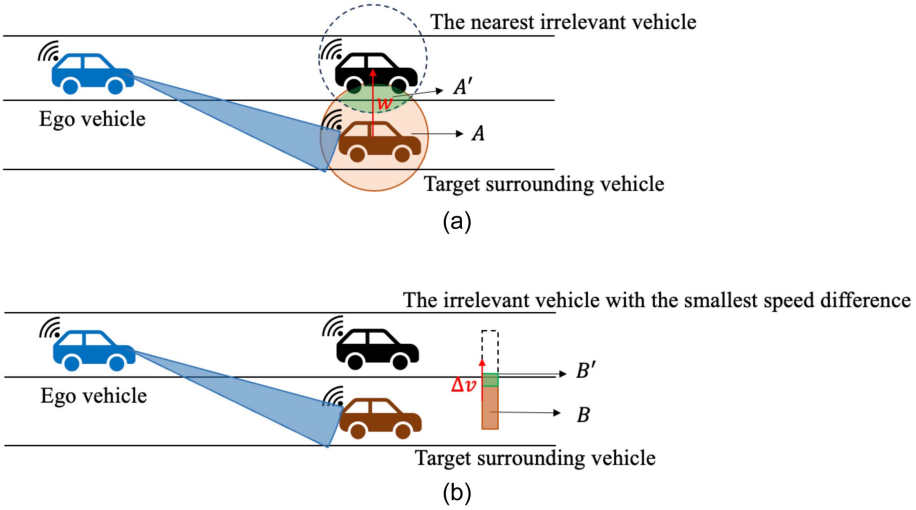

Fig. 4. Irrelevant vehicles for the target surrounding vehicle in position and speed: (a) irrelevant vehicle in possible distance region; and (b) irrelevant vehicle in possible speed region.

Radar distance measurement mainly depends on the time the signal returns (Cohen 2020). On the other hand, the radar's speed measurement is done by calculating the shift in frequency. Thus, these two events are independent.

The probability of the actual surrounding vehicle being identified as the connected vehicle in the position region is

$$P_{a,d} = 1 - (1 - (1 - \alpha_d)^n)^k \tag{10}$$

The probability of the actual surrounding vehicle being identified as the connected vehicle in the speed region is

$$P_{a,v} = 1 - (1 - (1 - \alpha_v)^n)^k \tag{11}$$

Then, by combining Eqs. (10) and (11), the probability of the actual surrounding vehicle identified as the connected vehicle is

$$P_a = P_{a,d} \times P_{a,v} \tag{12}$$

Error Rate Model

Depending on the radar distance and speed measurements, the search region would change. Given that the radar distance is more accurate than the GPS location-based distance, the radar distance error is assumed to be insignificant compared with the GPS distance error. The probability density function for the position of an irrelevant surrounding vehicle is defined as follows:

$$f(ex_g, ey_g) = \frac{1}{2\pi\delta^2} \exp\left(-\frac{ex_g^2 + ey_g^2}{\delta^2}\right) \tag{13}$$

where $\delta = \delta_x = \delta_y$. The probability of the irrelevant vehicle within Position region A for n measurements is

$$P_d = \left(\iint_{A'} f(ex_g, ey_g) \mathrm{d}ex_g \mathrm{d}ey_g\right)^n \tag{14}$$

$$A' = \{(ex_g \pm w)^2 + ey_g^2 < \delta^2 F^{-1}(\chi^2(2), 1 - \alpha_d)\} \tag{15}$$

where w = lane width; and A' = overlap of Region A and Region A's shift by w to the lateral direction. A' represents the possible region where the position of the nearest irrelevant vehicles falls in Region A to be identified as a candidate, as shown in Fig. 4(a). Region A' needs to be optimized to guarantee a low error rate.

Furthermore, the error associated with the GPS speed is negligible (Jain et al. 2021; Kubo 2009; Sadrieh et al. 2000; Serrano et al. 2004). For this reason, the GPS estimated speed error is deemed insignificant compared with the radar speed error

$$e_r^2 < \sigma_r^2 F^{-1}(\chi^2(1), 1 - \alpha_v) \tag{16}$$

The probability density function of its relative radar speed with respect to its actual speed is given by a normal distribution

$$f(e_r) = \frac{1}{\sqrt{2\pi\sigma_r^2}} \exp\left(-\frac{e_r^2}{\sigma_r^2}\right) \tag{17}$$

The probability of the speed of an irrelevant vehicle to be within the Speed region B for n measurements is

$$P_v = \left(\int_{B'} (f(e_r) de_r\right)^n \tag{18}$$

$$B' = \{(e_r \pm \Delta v)^2 < \sigma_r F^{-1}(\chi^2(1), 1 - \alpha_v)\} \tag{19}$$

where Δv = assumed smallest speed difference between the target preceding vehicle and the irrelevant nearby vehicle. Similar to Position region A' as shown in Fig. 4(b), B' is the possible region of the irrelevant vehicle Overlapping region B, which needs to be optimized to guarantee a low error rate. Here, $\Delta v = 0$ because the irrelevant vehicle may have the same speed as the surrounding target vehicle. Thus, the overall probability becomes

$$P_O = P_d \times P_v \tag{20}$$

At last, E_r, the probability that the nearest irrelevant vehicle as shown in Fig. 4, is determined to be the target connected surrounding vehicle in any of the k repetitions of the identification procedure, can be estimated based on the Binomial approximation as follows:

$$E_r = P_{\text{irr}} \approx 2kP_O \tag{21}$$

Table 2. Optimal values of n, k, α_d, and α_v as function of constraint parameters for the optimization problem [Eq. (22)]

Target error rate	t_{max}	P_{min}	W_1	W_2	n	k	α_d	α_v	Target unusability rate
10^{-10}	35	0.95	0.20	755	38	9	0.0196	0.0102	0.00326
10^{-8}			0.10	765	35	9	0.0184	0.0121	0.00137
10^{-6}			0.10	765	34	6	0.0110	0.0049	0.00096

Optimization Formulation and Optimized Parameters

Considering Eqs. (8)–(17), the following optimization problem, which ensures minimum surrounding target vehicle misidentification error and minimizes the cost of unusability error and time consumption, is formulated:

$$\text{Minimize } C = W_1(1 - P_a(\alpha_d, \alpha_v, n, k)) + W_2 \times nk\Delta T \quad (22)$$

Subject to

$$P_{irr} = 2k\left(\iint_{A'} f(ex_g, ey_g)\mathrm{d}ex_g\mathrm{d}ey_g\right)^n \times \left(\int_{B'} f(e_r)\mathrm{d}e_r\right)^n \le E_r \quad (23)$$

$$nk\Delta T \le t_{max} \quad (24)$$

$$P_a = [1 - (1 - (1 - \alpha_d)^n)^k] \times [1 - (1 - (1 - \alpha_v)^n)^k] \ge p_{min} \quad (25)$$

$$0 < \alpha_d, \qquad \alpha_v < 1 \quad (26)$$

where C = cost function, which consists of weighted unusability rate (Ur) and maximum time consumption with weights W_1 and W_2, respectively; n and k = positive integers for the times of matching shown in Fig. 2; and $nk\Delta T$ = time consumption when the time interval of each matching is ΔTs. In this paper, the time interval of each matching is set to be 0.1 s. The surrounding target vehicle misidentification error and the identification time are constrained to be less than the predefined values, E_r (i.e., a maximum error required to avoid an ego vehicle following an unconnected vehicle) and t_{max} (i.e., a maximum acceptable time consumption), respectively. The minimum acceptable usability of CACC is also constrained by a predefined value (p_{min}).

Due to the presence of nonlinear and integer constraints, a genetic algorithm (GA) is used to optimize for the parameters. Table 1 summarizes the weights and optimized parameter values of n, k, and α for the distance-only method under three levels of target misidentification error (E_r) of 10^{-6}, 10^{-8}, and 10^{-10}. Table 2 presents the weights and optimized parameter values of n, k, α_d, and α_v for the proposed ds-SVIS with the same three levels of E_r. The weights are different for ds-SVIS under $E_r = 10^{-6}$ from others for a low unusability rate.

Performance Evaluation

SVIS was evaluated using the real-world vehicle trajectories available from the Next Generation Simulation (NGSIM) data set to reproduce the traffic on a high-density highway segment. The ability of SVIS to identify connected and unconnected vehicles under various GPS and radar errors was investigated. The study examined a range of mixed traffic scenarios characterized by varying degrees of market penetration by connected vehicles, specifically 20%, 30%, 40%, 50%, 70%, 90%, and 100%. This approach was undertaken to evaluate the robustness of the SVIS in contexts with differing levels of traffic connectivity.

To model a particular market penetration, we independently assigned each vehicle in our simulation to be connected with the probability corresponding to that penetration. For example at a 30% market penetration, each vehicle in the simulation was assigned to be a connected vehicle with a probability of 0.3. The effectiveness of SVIS was investigated by considering observed vehicle misidentification error, observed unusability rate, and the time of identifying the target connected vehicle. It is essential to recognize that the observed misidentification error and unusability rate may differ from the target vehicle misidentification error and target unusability rate. This discrepancy arises due to variations in the assumed error distributions for GPS and radar, reflecting the potential uncertainties that can occur in real-world scenarios.

Data

The Federal Highway Administration (FHWA) Traffic Analysis Tools program conducted the NGSIM program and made the trajectory data available (Alexiadis et al. 2004). Here, 2,500 pairs of preceding/following vehicle data collected using high-resolution cameras from US Highway 101 (US 101) were utilized.

Sensor Error Consideration

This section of the study discusses the considered errors of GPS and radar sensors. The true distribution errors are typically unknown or varying with many factors (e.g., GPS, the number of available satellites, and nearby buildings).

Automotive Radar

For automated vehicles, millimeter-wave radar is one of the fundamental sensors. Bosch (Ludwigsburg, Germany) long-range radar (LRR) has been widely employed for ACC (Hasch et al. 2012). The Bosch long-range radar (LRR) specifications are 250 m detection range, 30° field of view, 0.1 m distance accuracy, 0.1 m/s speed accuracy, and 0.1° angle accuracy. Measurement errors were assumed to follow white noise (Ploeg et al. 2011).

However, products on the market suggest that range distance accuracies are around 10 cm and speed accuracies are generally less than 0.3 m/s (de Ponte Müller 2017; Klinefelter and Nanzer 2021). Therefore, for the evaluation of SVIS, a radar distance accuracy of 0.1 m was considered. However, because the speed accuracy can be up to 0.3 m/s, a sensitivity analysis for 0.1, 0.2, and 0.3 m/s was conducted.

GPS

The GPS with a pseudorange relative positioning approach can achieve an accuracy of 0.5–1.2 m on open highways (Liu et al. 2014; de Ponte Müller et al. 2014) and 2–6.5 m in dense urban environments (Alam et al. 2013; de Ponte Müller et al. 2014). The GPS errors were modeled as per Chen and Park (2022). The multipath effects are represented based on Giremus et al. (2007); specifically, we assumed that the multipath effect can be modeled by "abruptly adding biases with random magnitudes and durations to pseudo-range measurements." It was found that the speed error from Doppler measurements is under 10 cm/s in most cases (Kubo 2009).

Table 3. MOEs for d-SVIS (i.e., previous approach) and ds-SVIS (i.e., proposed approach) at different penetrations for different values of the target surrounding vehicle misidentification error rate (10 repetitions)

MOEs	Market penetration (%)	$E_r = 10^{-6}$		$E_r = 10^{-8}$		$E_r = 10^{-10}$	
		Distance	Distance and speed	Distance	Distance and speed	Distance	Distance and speed
Average observed misidentification error rate	20	1.7×10^{-3}	0.0	9.3×10^{-4}	**0.0**	**4.1×10^{-4}**	0.0
	30	1.2×10^{-3}	0.0	8.9×10^{-4}	**0.0**	**2.7×10^{-4}**	0.0
	40	1.2×10^{-3}	2.8×10^{-5}	4.3×10^{-4}	**0.0**	**2.7×10^{-4}**	0.0
	50	7.9×10^{-4}	0.0	3.3×10^{-4}	**0.0**	**3.2×10^{-4}**	0.0
	70	8.6×10^{-4}	0.0	2.1×10^{-4}	**0.0**	**9.2×10^{-5}**	0.0
	90	4.4×10^{-4}	0.0	5.5×10^{-5}	**0.0**	**1.0×10^{-7}**	0.0
	100	2.4×10^{-4}	0.0	1.9×10^{-5}	**0.0**	**9.7×10^{-6}**	0.0
Average observed unusability rate	20	0.068	0.041	0.058	**0.055**	**0.055**	0.060
	30	0.065	0.039	0.058	**0.051**	**0.057**	0.058
	40	0.064	0.035	0.055	**0.049**	**0.054**	0.056
	50	0.062	0.038	0.050	**0.050**	**0.052**	0.057
	70	0.060	0.034	0.049	**0.047**	**0.048**	0.053
	90	0.060	0.032	0.047	**0.045**	**0.046**	0.050
	100	0.057	0.032	0.045	**0.043**	**0.045**	0.049
Average time consumption (s)	20	2.36	3.84	3.98	**4.59**	**4.37**	4.92
	30	2.36	3.85	3.99	**4.57**	**4.39**	4.93
	40	2.39	3.86	4.00	**4.60**	**4.40**	4.95
	50	2.38	3.86	4.01	**4.60**	**4.42**	4.98
	70	2.39	3.87	4.03	**4.63**	**4.46**	5.01
	90	2.40	3.88	4.06	**4.66**	**4.49**	5.02
	100	2.40	3.89	4.08	**4.68**	**4.50**	5.05
Average	—	2.38	3.86	4.02	**4.62**	**4.43**	4.98

Note: Bold values represents the comparison between d-SVIS and ds-SVIS with maximum misidentification error rates in 10^{-8} and 10^{-10}, respectively.

Comparison of Distance-Only Method versus Distance and Speed Method

To evaluate whether the proposed method considering both distance and speed outperforms the distance-only method, especially in reducing the vehicle misidentification error and unusability rate, the following assumptions were made. The GPS and radar errors followed normal distributions with a mean of zero and different standard deviations, including GPS distance error of one, radar distance error of 0.1, GPS speed error of zero, and radar speed error of 0.1. A sensitivity analysis was conducted considering three levels of target vehicle misidentification errors (E_r) of 10^{-10}, 10^{-8}, and 10^{-6}.

Three measures of effectiveness (MOEs) were used for the comparative analysis. Table 3 compares the average of the observed vehicle misidentification error rates, observed unusability rate, and time consumption between the two approaches at different surrounding target vehicle misidentification errors. As indicated in Table 3, the ds-SVIS (proposed approach) outperformed the d-SVIS (previous approach). The average error rates were almost zero with the proposed approach.

Looking at the different surrounding target vehicle misidentification errors, $E_r = 10^{-6}$ had a rise in the error rate at the 40% market penetration rate for the proposed approach. GPS and radar distance and speed errors were randomly generated according to their corresponding distributions in each repetition. The investigations found that out of 10 replications, only one replication had a nonzero value. Then, simulations were run for 100 replications to observe the results. The observed vehicle misidentification error also showed some nonzero values. Thus, $E_r = 10^{-6}$ was deemed to be not acceptable for practical implementation. However, compared with the previous approach, it is still better than that of the $E_r = 10^{-10}$ level. Given that a close to zero vehicle misidentification error is required, the target vehicle misidentification error of 10^{-8} and 10^{-10} should be adopted with the proposed distance and speed approach.

The results indicated that at the target vehicle misidentification errors of $E_r = 10^{-8}$ and $E_r = 10^{-10}$, there was a slight variation in the unusability rate. At a target vehicle misidentification error of $E_r = 10^{-6}$, the unusability rate decreased, indicating a trade-off between observed vehicle misidentification error and unusability rate. To guarantee a low vehicle misidentification error, the search region needs to be small to exclude irrelevant vehicles, although a small search region could exclude the target vehicle and increase the unusability rate.

The average time consumption values indicated that more time is consumed using the distance and speed approach than by the distance-only approach for the same target vehicle misidentification error. Also, it has been validated from the cost of the optimization problem. From Table 3, a higher jump is attained at $E_r = 10^{-6}$. When looking at the average observed vehicle misidentification error in Table 3, it is higher for the distance only at $E_r = 10^{-6}$. Compared with E_r of other values, the required time consumption averages between the distance-only versus distance and speed increased to cover such a higher gap.

Table 3 also indicates that at $E_r = 10^{-6}$, the least time is consumed compared with E_r of other values for the proposed distance and speed approach. It is less than the time consumption averages of distance only for $E_r = 10^{-8}$ and $E_r = 10^{-10}$. Thus, compared with the previous distance-only approach, the proposed distance and speed approach also benefits the time consumption average if the results from $E_r = 10^{-6}$ having random nonzero values in observed vehicle misidentification error is acceptable. However, because lowering the average actual surrounding vehicle misidentification error, the parameter E_r of 10^{-8} and 10^{-10} with higher time consumption averages is preferred. At $E_r = 10^{-8}$, the distance and speed approach had similar time consumption as the distance-only approach when $E_r = 10^{-10}$, whereas the error rate of the

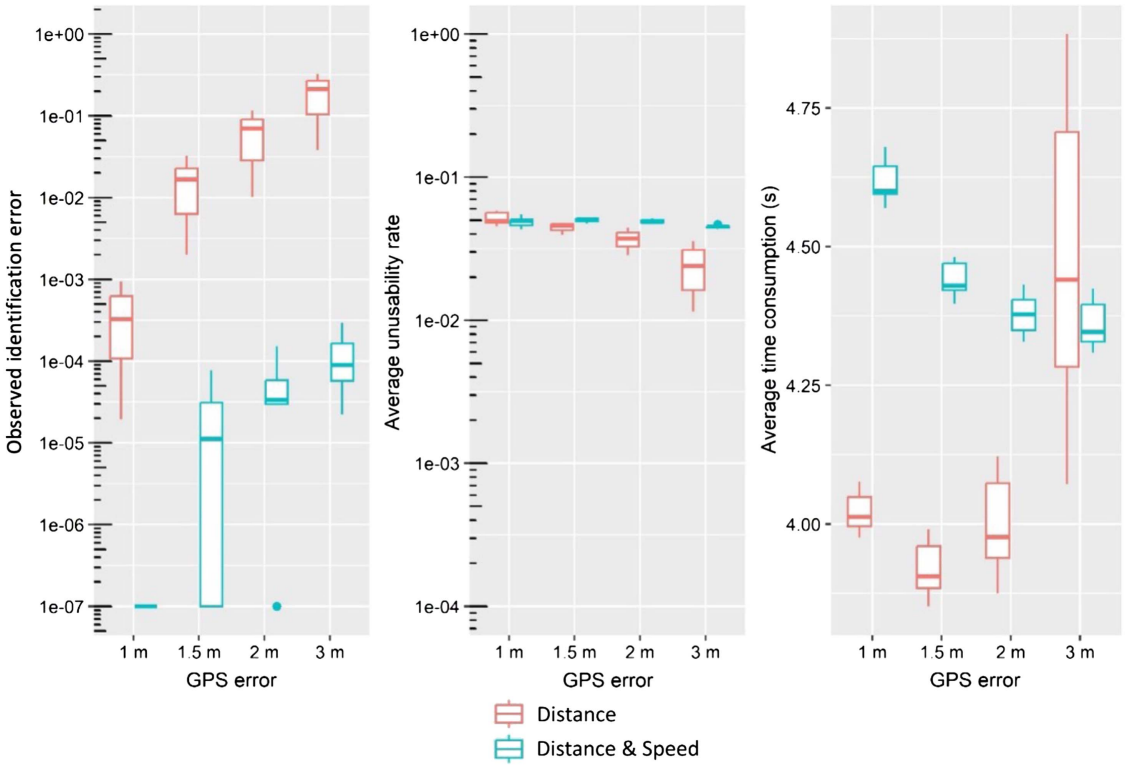

Fig. 5. Comparison of measure of effectiveness MOEs between distance (i.e., previous approach) versus distance and speed (i.e., proposed approach) at different GPS distance errors. Parameters refer to Tables 2 and 3.

proposed distance and speed approach at $E_r = 10^{-8}$ was lower than that of the distance-only approach at $E_r = 10^{-10}$.

Thus, Table 3 demonstrates that the proposed distance and speed approach is more advantageous than the previous distance-only approach in terms of average error rate, average unusability rate, and average time consumption. Out of the three error rates evaluated, we selected $E_r = 10^{-8}$ for the proposed distance and speed approach for further investigation. This is because it provides a similar error rate and unusability, but slightly shorter time than that of $E_r = 10^{-10}$ cases.

Comparison of GPS Sensitivity of Distance-Only versus Distance and Speed

With the selection of $E_r = 10^{-8}$, this section analyzed the sensitivity of GPS distance following a normal distribution with the standard radar distance error of 0.1, neglectable GPS speed error, and both standard radar distance and speed error of 0.1. Usually, the standard GPS distance error is one, which can be propagated quickly based on different errors, e.g., multipath effect (Chen and Park 2022). Regarding the standard radar speed error, it can be 0.1, but some companies' radar has a standard speed error of 0.3 (de Ponte Müller 2017). Therefore, the focus was only on the different GPS distance errors.

The comparisons of MOEs between the previous distance-only versus the proposed distance and speed approaches at different GPS distance errors are shown in Fig. 5. The analysis focused on, i.e., target vehicle misidentification error and time consumption because the unusability rate does not change significantly when ds-SVIS is introduced. Specifically, for the standard GPS distance error of one, the difference was not statistically significant (p-value = 0.1696). In addition, the standard GPS distance error should be one or below to minimize the surrounding vehicle misidentification error. With the standard GPS distance error of 1.5, the proposed approach could show a 10^{-4} surrounding vehicle misidentification error.

GPS Distance and Radar Speed Sensitivity for the Distance and Speed Approach

This part analyzed the sensitivity of the GPS distances and radar speeds for ds-SVIS. The standard radar speed error was assumed to be 0.1, and the GPS speed error is insignificant.

Fig. 6 compares the average observed misidentification error rate, average unusability rate, and average time consumption for the distance and speed approach (i.e., ds-SVIS) at different GPS distance errors and radar speed errors.

Because safety is the most critical, the surrounding vehicle misidentification error should be minimized. In order to maintain the observed vehicle misidentification error close to 10^{-8}, the standard radar speed error should be 0.2 or below. With a standard GPS distance error of one, the unusability errors and time consumption are reasonable.

Conclusions and Recommendations

Based on the simulations conducted in this research, the following conclusions are made:

- The proposed ds-SVIS approach is more efficient than the previous d-SVIS. Considering the base errors, the average observed vehicle misidentification errors were zero for the proposed approach when $E_r = 10^{-8}$ and 10^{-10}. On the contrary, the previous approach resulted in nonzero error even when $E_r = 10^{-10}$. Given that the proposed approach under $E_r = 10^{-6}$ showed nonzero error, E_r should be smaller than 10^{-6}.
- The unusability errors were largely consistent regardless of the E_r values, and the previous or proposed approaches. Again, this

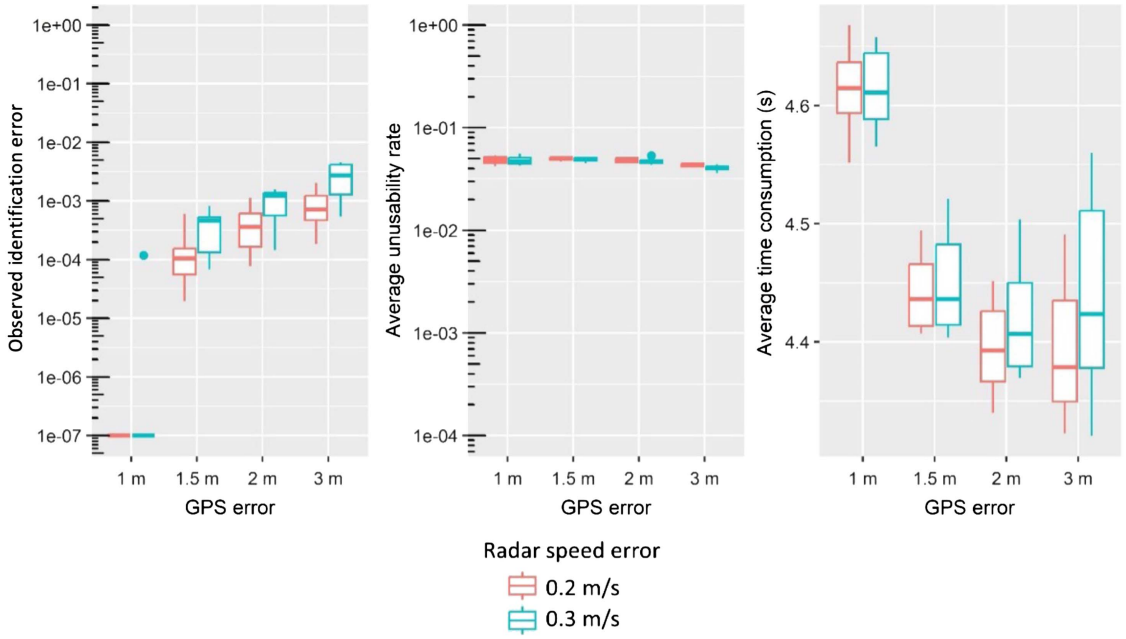

Fig. 6. Comparison of measure of effectiveness MOEs at different GPS distance and radar speed errors for distance and speed (i.e., proposed approach). Parameters refer to Tables 2 and 3.

unusability error is not safety-critical because the ego vehicle would implement adaptive cruise control instead of cooperative adaptive cruise control.

- Based on the sensitivity analyses on the GPS distance error and radar speed error, the proposed approach with a standard GPS error of one or below and standard radar speed error of 0.2 or below should be considered to ensure the observed surrounding vehicle misidentification error is close to 10^{-8}.

The following recommendations are made for future research and real-world implementation: First, implement the proposed approach (ds-SVIS) with $E_r = 10^{-8}$ to form CACC and demonstrate the benefits that it would bring in highway scenarios. Second, investigate the usefulness of SVIS on uncongested highways and urban corridors, and expand the SVIS for additional connected vehicle applications such as cooperative merges and cooperative lane changes. Third, future studies should consider field testing and collecting data with different vehicle manufacturers in different weather and roadway environments (e.g., roadway gradients, inclement weather conditions, and so on).

Data Availability Statement

All data, models, and code generated or used during the study appear in the published article.

Acknowledgments

This research is supported by the National Science Foundation (NSF) under Grant No. CMMI-2009342 and Toyota Motor North America R&D. This paper's contents reflect the authors' views, who are responsible for the facts and accuracy of the data presented herein.

Author contributions: B. Park: Study conception and design, Analysis and interpretation of results. S. Avedisov: Study conception and design, Analysis and interpretation of results. M. Imran: Simulation setup and implementation, Analysis and interpretation of results, Writing–original draft. Z. Mu: Simulation setup and implementation, Analysis and interpretation of results, Writing–original draft. All authors reviewed the results and approved the final version of the manuscript.

Notation

The following symbols are used in this paper:

A = Search region A with respect to distance;
A' = nearest irrelevant vehicles possible region;
B = Search region B with respect to speed;
B' = irrelevant vehicles with the smallest speed difference possible region;
d = distance between two nearby vehicles (m);
E_r = target vehicle misidentification error rate;
e = speed error (m/s);
ex = distance error of longitudinal gap (m);
ey = distance error of lateral gap (m);
k = outer loops of unconnected vehicle identification;
n = inner loops of connected vehicle identification;
P_a = probability of the actual connected vehicle to be identified as the connected vehicle;
$P_{a,d}$ = probability of the actual connected vehicle to be identified as the connected vehicle with respect to the distance (position) region;
$P_{a,v}$ = probability of the actual connected vehicle to be identified as the connected vehicle with respect to the speed region;
P_d = probability of an irrelevant vehicle is within search region A of position;
P_{irr} = probability of an irrelevant vehicle is identified as the connected vehicle;
P_O = overall probability of an irrelevant vehicle is within Search regions A and B;
P_v = probability of an irrelevant vehicle is within Search region B of speed;

$p_{\min}$ = minimum acceptable usability;
t = time (s);
$t_{\max}$ = maximum acceptable time consumption (s);
U_r = target unusability rate;
v = speed of vehicle (m/s);
W = weights of objective functions;
w = width of the road (m);
α = probability that the actual surrounding connected vehicle is positioned outside the search region;
δ^2 = squared sum of independent, standard normal variables follows Chi-square (χ^2) distribution; and
σ = standard derivation of error.

References

Alam, N., A. Kealy, and A. G. Dempster. 2013. "An INS-aided tight integration approach for relative positioning enhancement in VANETs." *IEEE Trans. Intell. Transp. Syst.* 14 (4): 1992–1996. https://doi.org/10.1109/TITS.2013.2265235.

Alexiadis, V., J. Colyar, J. Halkias, R. Hranac, and G. McHale. 2004. "The next generation simulation." *Inst. Transp. Eng.* 74 (8): 22–26.

Bajpai, J. N. 2016. "Emerging vehicle technologies & the search for urban mobility solutions." *Urban Plann. Transport Res.* 4 (1): 83–100. https://doi.org/10.1080/21650020.2016.1185964.

Bansal, P., and K. M. Kockelman. 2017. "Forecasting Americans' long-term adoption of connected and autonomous vehicle technologies." *Transp. Res. Part A Policy Pract.* 95 (Dec): 49–63. https://doi.org/10.1016/j.tra.2016.10.013.

Chen, Z., and B. B. Park. 2020. "Preceding vehicle identification for cooperative adaptive cruise control platoon forming." *IEEE Trans. Intell. Transp. Syst.* 21 (1): 308–320. https://doi.org/10.1109/TITS.2019.2891353.

Chen, Z., and B. B. Park. 2022. "Connected preceding vehicle identification for enabling cooperative automated driving in mixed traffic." *J. Transp. Eng. A Syst.* 148 (5): 04022013. https://doi.org/10.1061/JTEPBS.0000661.

Cohen, J. 2020. "How RADARs work–A look at radio detection and ranging." *Think Autonomous*. Accessed July 19, 2022. https://www.thinkautonomous.ai/blog/how-radars-work/.

Deng, J., L. Yu, Y. Fu, O. Hambolu, and R. R. Brooks. 2017. "Security and data privacy of modern automobiles." In *Data analytics for intelligent transportation systems*, 131–163. Amsterdam, Netherlands: Elsevier.

de Ponte Müller, F. 2017. "Survey on ranging sensors and cooperative techniques for relative positioning of vehicles." *Sensors* 17 (2): 271. https://doi.org/10.3390/s17020271.

de Ponte Müller, F., E. M. Diaz, B. Kloiber, and T. Strang. 2014. "Bayesian cooperative relative vehicle positioning using pseudorange differences." In *Proc., Record - IEEE PLANS, Position Location and Navigation Symp.*, 434–444. Piscataway, NJ: Institute of Electrical and Electronics Engineers.

Geiger, A., M. Lauer, F. Moosmann, B. Ranft, H. Rapp, C. Stiller, and J. Ziegler. 2012. "Team AnnieWAY's entry to the 2011 grand cooperative driving challenge." *IEEE Trans. Intell. Transp. Syst.* 13 (3): 1008–1017. https://doi.org/10.1109/TITS.2012.2189882.

Giremus, A., J. Y. Tourneret, and V. Calmettes. 2007. "A particle filtering approach for joint detection/estimation of multipath effects on GPS measurements." *IEEE Trans. Signal Process.* 55 (4): 1275–1285. https://doi.org/10.1109/TSP.2006.888895.

Hasch, J., E. Topak, R. Schnabel, T. Zwick, R. Weigel, and C. Waldschmidt. 2012. "Millimeter-wave technology for automotive radar sensors in the 77 GHz frequency band." *IEEE Trans. Microwave Theory Tech.* 60 (3): 845–860. https://doi.org/10.1109/TMTT.2011.2178427.

Jain, A., D. Kulemann, and S. Schon. 2021. "Improved velocity estimation in urban areas using Doppler observations." In *Proc., 2021 Int. Conf. on Localization and GNSS (ICL-GNSS)*. Piscataway, NJ: Institute of Electrical and Electronics Engineers.

Kim, N., M. Duoba, N. Kim, and A. Rousseau. 2013. "Validating volt PHEV model with dynamometer test data using Autonomie." *SAE Int. J. Passenger Cars Mech. Syst.* 6 (2): 985–992. https://doi.org/10.4271/2013-01-1458.

Klinefelter, E., and J. A. Nanzer. 2021. "Automotive velocity sensing using millimeter-wave interferometric radar." In Vol. 69 of *Proc., IEEE Transactions on Microwave Theory and Techniques*, 1096–1104. New York: IEEE.

Kubo, N. 2009. "Advantage of velocity measurements on instantaneous RTK positioning." *GPS Solutions* 13 (4): 271–280. https://doi.org/10.1007/s10291-009-0120-9.

Lioris, J., R. Pedarsani, F. Y. Tascikaraoglu, and P. Varaiya. 2017. "Platoons of connected vehicles can double throughput in urban roads." *Transp. Res. Part C Emerging Technol.* 77 (Dec): 292–305. https://doi.org/10.1016/j.trc.2017.01.023.

Liu, K., H. B. Lim, E. Frazzoli, H. Ji, and V. C. S. Lee. 2014. "Improving positioning accuracy using GPS pseudorange measurements for cooperative vehicular localization." *IEEE Trans. Veh. Technol.* 63 (6): 2544–2556. https://doi.org/10.1109/TVT.2013.2296071.

Milanes, V., S. E. Shladover, J. Spring, C. Nowakowski, H. Kawazoe, and M. Nakamura. 2014. "Cooperative adaptive cruise control in real traffic situations." *IEEE Trans. Intell. Transp. Syst.* 15 (1): 296–305. https://doi.org/10.1109/TITS.2013.2278494.

Naus, G. J. L., R. P. A. Vugts, J. Ploeg, M. J. G. van de Molengraft, and M. Steinbuch. 2010. "String-stable CACC design and experimental validation: A frequency-domain approach." *IEEE Trans. Veh. Technol.* 59 (9): 4268–4279. https://doi.org/10.1109/TVT.2010.2076320.

Ploeg, J., B. T. M. Scheepers, E. van Nunen, N. van de Wouw, and H. Nijmeijer. 2011. "Design and experimental evaluation of cooperative adaptive cruise control." In *Proc., IEEE Conf. on Intelligent Transportation Systems*, 260–265. New York: IEEE.

Rajamani, R., and S. E. Shladover. 2001. "An experimental comparative study of autonomous and co-operative vehicle-follower control systems." *Transp. Res. Part C Emerging Technol.* 9 (1): 15–31. https://doi.org/10.1016/S0968-090X(00)00021-8.

Sadrieh, S. N., A. Broumandan, and G. Lachapelle. 2000. "Doppler characterization of a mobile GNSS receiver in multipath fading channels." *J. Navig.* 65 (3): 477–494. https://doi.org/10.1017/S037346331200015X.

Serrano, L., D. Kim, R. B. Langley, K. Itani, and M. Ueno. 2004. "A GPS velocity sensor: How accurate can it be? A first look." In *Proc., 2004 National Technical Meeting of the Institute of Navigation*, 875–885. Manassas, VA: Institute of Navigation.

Shladover, S. E., D. Su, and X.-Y. Lu. 2012. "Impacts of cooperative adaptive cruise control on freeway traffic flow." *Transp. Res. Rec.* 2324 (1): 63–70. https://doi.org/10.3141/2324-08.

V2X Core Technical Committee. 2016. *Dedicated short range communications (DSRC) message set dictionary.* Warrendale, PA: Society of Automotive Engineers.

Wang, D., M. Hu, Y. Wang, J. Wang, H. Qin, and Y. Bian. 2016. "Model predictive control–based cooperative lane change strategy for improving traffic flow." *Adv. Mech. Eng.* 8 (2): 1687814016632992. https://doi.org/10.1177/1687814016632992.

Yao, Z., B. Zhao, T. Yuan, H. Jiang, and Y. Jiang. 2020. "Reducing gasoline consumption in mixed connected automated vehicles environment: A joint optimization framework for traffic signals and vehicle trajectory." *J. Cleaner Prod.* 265 (Jun): 121836. https://doi.org/10.1016/j.jclepro.2020.121836.

Zheng, Y., B. Ran, X. Qu, J. Zhang, and Y. Lin. 2020. "Cooperative lane changing strategies to improve traffic operation and safety nearby freeway off-ramps in a connected and automated vehicles environment." *IEEE Trans. Intell. Transp. Syst.* 21 (11): 4605–4614. https://doi.org/10.1109/TITS.2019.2942050.